CoA Memo. No. 164

September, 1968

THE COLLEGE OF AERONAUTICS

DEPARTMENT OF MATERIALS

# Extended plasticity in commercial-purity zinc

- by -

D.A.C. Williams,* H. Naziri** and R. Pearce**



## SUMMARY

90% rolling-reduction of annealed commercial-purity zinc sheet (grain size 100 - 150 μ) results in the fragmentation of the large grains into, finally, stable micro-grains, 1 - 2μ in diameter. The stability of the micro-grains is due to the presence of soluble and insoluble impurities which prevent recrystallization.

This micro-grain material is strain-rate sensitive, and elongations of 200% have been obtained at room temperature.

Although this as-rolled, 90% reduction zinc sheet is not super-plastic according to the current definition, its behaviour has led to the coining of the phase 'extended plasticity'.

Evidence of grain-boundary sliding is found on examination of the surface by scanning electron microscopy, while the examination of thin foils and activation energy measurements support the dynamic softening (recovery) theory; thus, both these mechanisms must be operating, to a greater or less extent, to confer on this material the observe mechanical behaviour.

It is finally concluded that it is dangerous to draw conclusions regarding the mechanism of plastic deformation from surface observations alone.

---

* Investigator: Fulmer Research Institute (Bucks).

** H. Naziri, Department of Materials, The College of Aeronautics, Cranfield.
R. Pearce, Department of Materials, The College of Aeronautics, Cranfield.

## Introduction

A number of papers have appeared on the mechanical and microstructural behaviour of polycrystalline zinc and dispersion-strengthened zinc alloys.

Chadwick (1) found that the physical properties of rolled zinc were subject to considerable variation due to the presence of impurities. Electrolytically-pure zinc, rolled 80% was observed to recrystallize completely after one month at room temperature (the impurities iron, lead and cadmium were all less than 0.005%). The addition of 0.02% of iron or magnesium was found to prevent recrystallization.

Ramsey (2) tested hot-rolled zinc sheets of 99.99% purity and found that sub-grains tended to form, both at elevated temperatures and slow strain-rates. In the process of straining the as-rolled material, at 250°C, recrystallization occurred at 5% elongation. At 200°C, the zinc deformed either by slip or by the formation of a sub-structure and its movement, which ever was energetically favourable to the individual grains, the sub-structure being prominent at high temperatures and slow strain rates.

McCarthy (3) prepared zinc and zinc alloys by a powder metallurgical technique. He observed a 'dispersion softening' effect, an increase in ductility for a 15 vol % tungsten alloy compared with pure zinc. These tests were done at room temperature.

This enhanced plasticity was explained on the basis of strain-induced vacancy-formation, stress-distribution effects and fineness of the slip bands.

Tromans and Lund (4) prepared zinc-zinc oxide alloys by a very similar powder metallurgical technique. Enhanced plasticity was observed at room temperature in the Zn-ZnO alloy. Grain-boundary sliding and migration was concluded to be the effective deformation mechanism. The object of the present work is to study some similar phenomena observed in the course of other work on commercial-purity zinc sheet and to attempt to elucidate the deformation mechanism involved.

## Material

The material used was commercial-purity zinc supplied by R.T.Z. Ltd., in the form of plate 0.192 in. thick. A spectrographic analysis recorded the following:

| Pb | Cd | Fe | Cu | Al | Ti | Mg | |
|---|---|---|---|---|---|---|---|
| 0.8 | 0.05 | 0.02 | 0.002 | 0.001 | 0.001 | 0.001 | % |

## Experimental procedures

### Material Processing and Tensile Testing:

Supplied 5.5 in x 5.5 in x 0.192 in. plates were machined on both faces to a thickness of 0.175 in. The plates were rolled at room temperature in a 'Stanat-Mann' two-high mill. The rolls were $5\frac{1}{2}$ in. in diameter, and the rolling speed was 25 ft/min.

Tensile-test specimens were machined in a 'Tensilkut' machine. The specimen-gauge length was 2.5 in/0.5 ± .001 in.

Tensile tests were done in an Instron testing machine at crosshead speeds varying from 0.002 to 20.0 in/min.

For tests above room temperature an air-circulating oven was modified to fit in the Instron machine and enclose specimen extensions up to 250%. The temperature was controlled within ± 1.5°C.

### Metallography

#### Optical

The surface of the tensile specimens were examined without using a mounting medium. Electropolishing with the 'Ellopol' apparatus and a proprietary electrolyte, suitable for zinc, was used. The voltage was kept sufficiently low (20/25v) to prevent excessive heating.

An etching technique due to Chadwick (1) was found to be satisfactory. A large drop of fuming nitric acid was placed on the surface, and about 5 seconds later a drop of distilled water allowed to make contact at the edge of the nitric acid pool. The subsequent reaction was immediately quenched under the tap and the area opposite to that at which the water was introduced was found suitable for study under the microscope.

For the examination of sections, the specimens were mounted in a cold-setting plastic. The microstructure was observed up to a magnification of X2000 using an oil-immersion lens.

#### Scanning electron microscopy

To study the topographical nature of the surface, electropolishing was carried out before straining, followed by examination using a Cambridge Instruments Ltd., scanning electron microscope.

#### Electron probe micro-analysis

To obtain the distribution of any second-phase particles in the zinc matrix, micro-analysis was done on an Cambridge Instruments Ltd., electron probe.

Transmission, thin-film electron microscopy

Specimens for thin-film electron microscopy were thinned by a two-stage thinning technique.

2.30 mm diameter and 0.008 in. thick discs were spark machined and dimpled from both sides to a thickness of 0.002 in. The final thinning was done using an electropolishing solution - 375 c.c. orthophosphoric acid in 625 c.c. ethanol - at room temperature, and 10 - 12 volts potential difference.

Results

Mechanical

Rolling: The zinc shows an unusual behaviour during rolling. Fig. 1 shows the Vickers hardness vs. percentage reduction and a continual decrease in hardness is obtained. Fig. 2 shows that ageing of the as-rolled material occurs; several days are required before an equilibrium condition is reached. In the first 1000 hours the tensile strength increases from $20 \times 10^3$ p.s.i. to $25 \times 10^3$ p.s.i., and the hardness from 40 $H_v$ to 60 $H_v$. To avoid any discrepancies due to variation in properties on ageing, the material was allowed to stand at least three days before testing.

Tensile tests: Fig. 3 shows the effect of rolling on uniform elongation ($e_u$). It will be seen that below 50% reduction $e_u$ is in the range 15-19%, while over 50%, the uniform elongation rises to 70% increasing finally to 120%. All these tests were carried out at a crosshead speed of 0.2 in/min.

The effect of speed of testing on total elongation ($e_t$) for different percentage reductions is shown in Fig. 4. At the slow speed, the increase in $e_t$ with percentage reduction can be seen, even though the crosssection of the test piece is diminishing. At the higher speed, the reduction in $e_t$ indicates an increasing strain-rate sensitivity with increasing rolling reduction.

An effect of annealing is shown in Fig. 5. Speed of testing has virtually no effect on the total elongation for material rolled and then recrystallized (5 min. at 200°C).

Fig. 6 shows the effect of crosshead speed on zinc rolled 80%. Annealed material exhibits virtually no strain-rate sensitivity, while this is not so for the as-rolled material. To determine the strain-rate sensitivity exponent (m), and activation energy (Q), material rolled to 90% reduction were used. Fig. 7 shows the true stress - true strain curves at room temperature for various crosshead speeds. The curves are characteristic of those for the hot working of metals in torsion. The stress increases rapidly at first to a peak, falling a little, and gradually reaching a steady-state region before fracture. The peak and its width being dependent on (16) the strain-rate and temperature of testing.

The stress-strain curve of a material which exhibits strain-rate sensitivity may be represented by the relationship:

$$\sigma = K\dot{\epsilon}^m$$

where $\sigma$ is the true stress, $\dot{\epsilon}$ is the true strain-rate, m the strain-rate sensitivity exponent and k a constant. The m-value is obtained from:

$$m = \delta(\ln\sigma)/\delta(\ln\dot{\epsilon})$$

and a value of m = 0.2 was obtained for the as-rolled 90% reduced material at 0.43 Tm. In the case of the recrystallized zinc a m-value of 0.06 was obtained. For superplastic materials, m may be as high as 0.5; m = 1 is the condition for pure Newtonian flow.

The determination of the activation energy (Q), at constant stress, was obtained from the relationship proposed by Sellars and Tegart (5):

$$\dot{\epsilon} = A(\sinh \alpha\sigma)^{n'} \exp(^{-Q}/RT),$$

where A, $\alpha$, n' are temperature independent constants. Results obtained from the torsional hot-working of a number of metals fit closely to this relationship (17).

The activation energy, was obtained from a plot of log $\dot{\epsilon}$, at constant sinh $\alpha\sigma$, against 1/T (Fig. 8). This plot gave a Q-value of 21.5 $\pm$ 1k cal/mole (Fig. 9).

## Microstructures

### Optical microscopy

The original annealed material is shown in Fig. 10. This is typical of commercial purity zinc, with an average grain size of 100-150$\mu$ and lead stringers indicating the rolling direction. Lead is virtually insoluble in zinc. The change in microstructure on rolling to 90% reduction is in Fig. 10. The initially recrystallized grains become increasingly fragmented until a very fine micro-grain of 1-2$\mu$ in size is obtained.

To observe the effect of strain-rate on microstructure, specimens of as-rolled, 90% reduction, and as-rolled 90% reduction and recrystallized were strained at crosshead speeds of 0.2 in/min and 20 in/min. Fig. 11 shows the as-rolled material deformed and undeformed. The grain size has approximately doubled during slow-speed deformation and it has retained its roughly equiaxed grains (Fig. 11)(X3000). The lead stringers are more fragmented after slow-speed than high-speed deformation (Fig. 11)(X1000).

Fig. 12 (X200) shows the recrystallized material before deformation and after tensile straining at high and low speeds of failure. Grain deformation is evident, and the lead stringers appear more prominent after deformation.

The structure appears more 'disturbed' after high speed deformation. With the material rolled 90%, the longitudinal, transverse and surface microstructures were all very similar. An electropolished, unetched, surface was examined after straining in increments of 5% elongations. With increasing strain, grain boundaries become visible and the grains were found to be out of focus relative to each other; an indication of the variation in the surface height of grains.

Electron probe micro-analysis

Fig. 13 shows the distribution of lead particles in the zinc matrix; lead being the major impurity in this alloy. Lead in a very fine form is randomly distributed throughout the microstructure while some of the large agglomerates still remain.

Scanning electron microscopy

Samples of recrystallized material, strained to fracture at 0.02 in/min. and 2 in/min. were examined, and Fig. 14 shows the recrystallized material strained at the crosshead speed of 0.02 in/min. Slip lines are evident, fracture appears to be initiated at the grain boundary triplepoints and the crack progresses along the boundaries.

Fig. 15 shows the recrystallized material strained at the higher crosshead speed of 2 in/min. Here, slip lines are again evident, but on a finer scale, and duplex slip seems to have taken place. Fracture, again appears to start at the triple points and progresses along the boundaries. Before straining the as-rolled specimens, the electropolished surface was scratched with $^{1}/_{4}$ $\mu$ diamond paste in an attempt to observe grain boundary displacement, if any. Surface of the specimens were examined after straining at three crosshead speeds - 0.02 in/min., 2 in/min. and 20 in/min. Fig. 16 shows the displacement of scratches with the specimen strained at 2 in/min. to an elongation of 50%, due to the relative movement of the adjacent grains. Cavity formation at the grain boundaries is also evident.

Fig. 17 shows a specimen strained at a slower speed (0.02 in/min.) and to a higher elongation (100%).

Here, scratches are displaced due to extensive movement by the grains, but the scratches in this case appear to be less well-defined. Also, there is evidence that a number of grains move as a 'unit' before separating and moving individually. The vertical grain displacement and the extensive void formation are quite remarkable.

Fig. 18 shows a specimen strained at a very high speed (20 in/min) to fracture. An elongation of only 20% was obtained. Fig. 18 (X100) shows fibrous cracking perpendicular to the direction of straining and at higher magnification Fig. 18 (X10,000) intergranular fracture appears to have taken place. Lack of grain movement is apparent.

In further tests, specimens were strained to fracture, at a fixed crosshead speed of 0.2 in/min and at different temperatures (-196°C, -55°C, 0°C, 20°C and 70°C). Virtually no elongation was obtained at temperatures of -196°C and -55°C. Fig. 19 shows the lack of grain movement. However, voids at the grain boundary triple points are evident. Increasing the temperature of testing gives higher elongations, and microstructurally, there appears to be an increase in grain size, grain movement and void formation, Fig. 20.

No evidence of slip is observed under any condition when testing the as-rolled material; this is borne out in Fig. 21. A recrystallized grain in a micro-grain matrix was formed by local heating during electropilishing. The recrystallized grain has deformed by slip, while the movement of the micro-grains is indicated by the void formation and cracking along the grain boundaries.

Transmission thin-film electron microscopy

Figs. 22 and 23 (X42,000) shows the micrograph of the as-rolled, 90% reduction and as-rolled recrystallized materials. The black spots are impurity particles, probably lead. In both the cases the particles are present at the grain boundaries and in the grains. Fig. 22 (X21,000) is a micrograph of the as-rolled material at a lower magnification and it should be noted that the grains are not quite equiaxed. No dislocation networks were observed, though in a number of cases a few dislocation lines were seen.

Fig. 24 is a micrograph of the as-rolled material, but strained 100% at room temperature. The particles are still observed to be present at the grain boundaries and in the grains. However, the grains have grown in size and become equiaxed compared with the as-rolled starting material. Again, no dislocation networks were observed.

Discussion

In the present work, recrystallized grains, room temperature rolled to 90% reduction, break down to give micro-grains 1 to 2$\mu$ in size. Subsequent recrystallization of the as-rolled material is prevented by the impurities (1). The transition in properties during grain fragmentation is demonstrated by the change in hardness and elongations with percentage reduction (Figs. 1 and 3); 40 to 50% reduction appears to be critical and possibly some change in deformation mechanism occurs at this reduction.

Room temperature corresponds to $\sim 0.43\ T_m$ for zinc. However, as heat is generated in the rolling process there must be a stage, as no cooling

was introduced, where the metal is well above this value and is thus being 'hot rolled'. Immediately after cooling, extreme softness of the sheet is very noticeable though this, of course, passes with time. It is suggested that the grain size finally produced by this rolling procedure is due to the pinning of the substructure formed by the impurity particles and the size controlled by the particle spacing. Fine particles in a dislocation matrix have been found to be responsible for a cell-structure of this type (7).

Johnson (6) has divided superplastic materials into two classes (1) those which are in a special structural condition i.e. fine grain size and containing one or more second phases, and (2) those for which special testing conditions are needed, i.e. temperature cycling or some other means required to make a phase boundary move through a strained material.

The behaviour of this zinc approximates to the special-structural superplasticity and so it should belong to class 1.

Controversy exists as to the deformation mechanism responsible for the superplastic behaviour exhibited by the class 1 materials Two models which have received support are: a) grain boundary sliding and migration, and b) a dynamic softening process in the form of dynamic recovery and/or dynamic recrystallization.

In the first model, a) it is considered that at very high strain-rates or low temperatures the conventional deformation proceses (slip, twinning and fracture) operate but with a decrease in strain-rate thete is a transition to grain boundary sliding and migration (8,9,10,11,12 and 13).

The requirement for maximum ductility on the grain boundary sliding and migration model is very small grain size, i.e. an increase in grain boundary area per unit volume so that an increase in sliding area is obtained.

A number of workers (10,11,13) have opted for this model after observing metallographically the displacement of scratches. Furthermore, as voids were not observed at the grain junctions, it was concluded that grain boundary migration was the accommodating process. In addition the appearance of the grains - equiaxed, and rounded has been given as corroborative evidence (12).

In the present work, Fig. 16, shows micrographic evidence of grain boundary sliding. The scratches and displaced grains protrude from the surface. However, extensive void formation with increase in strain is evident. Further, the greater the straining, the greater is the micro-rumpling of the surface and the disappearance of the scratches (Fig. 17). Migration which is generally considered to be the accommodating process to obviate void formation is evidently absent, and it must be concluded that sliding is taking place, whereas migration is not.

Figure 24 is a transmission thin-film micrograph of 90% as-rolled material subsequently strained 100% in tension. Here there is no evidence of void formation, though the grains have become rounded, and equiaxed. In addition, the grains have approximately doubled in size while particles are still situated both at the grain boundaries and in the grains.

Can these effects be fitted to the grain boundary sliding and migration model? Stevens (14) has proposed a method for the quantitative measurement of the strain contributed by grain boundary sliding to the total strain, but the application of this approach was tried unsuccessfully by Holt (13) at elongations in excess of 50%, due to excessive surface rumpling. In the present work also, the scratches tended to disappear at the higher strains. Holt concluded that the error in computing the fraction of grain boundary sliding strain to total strain was of the order of $\pm$ 30%. Again, in the present work, particles are situated in the grain boundaries, both before and after deformation, and these will not be compatible with grain boundary movement (15).

It has also been found that, by decreasing the temperature, or increasing the strain rate, ductility is drastically reduced. A specimen (Fig. 19) examined after testing at - 196°C and crosshead speed of 2.0 in/min did not show any slip lines; even though slip has been put forward as the deformation mechanism under these conditions. No slip-lines are again evident in the micro-grains (Fig. 21) though the recrystallized grain in the matrix of micro-grains does show slip-lines. It is possible that slip is occurring, but that the slip-lines are so fine that their resolution is not possible (13).

Fig. 18 shows that the as-rolled material, strained at room temperature and crosshead speed of 20 in/min. This has fractured in a 'fibrous' manner when viewed at a magnification of 100 times, while cracks are clearly intergranular at high magnification (X10,000) (Fig. 18).

In model (b), the dynamic softening model, superplasticity is considered as a phenomenon exhibited while working the material in the region of 0.5 Tm, and the ability of the softening processes to balance the strain hardening processes.

By the operation of a dynamic softening process sufficiently rapid to balance strain hardening, large strains in torsion can be obtained (16, 17). Dynamic softening can be divided into dynamic recovery and dynamic recrystallization, and the experimental evidence supporting these processes in the present results will be considered. During rolling the zinc sheet, the dislocation density increases and a sub-structure begins to form. At a steady state, all other factors remaining constant, a disintegration and reformation of the dislocation arrays at the equilibrium spacing - sub-structure occurs.

Due to the large number of small particles in the matrix, inevitably, at the equilibrium spacing, the boundaries will be pinned by some of these particles.

Once a equilibrium boundary-spacing is obtained, further dislocations generated are annihilated at the sub-boundaries in a climb-controlled process (17). The presumed constancy of dislocations of opposite signs from adjacent grains cancel each other out, in the sub-boundaries.

On rolling, an increase in the reduction merely repeats these processes, the particles consolidating each new equilibrium spacing. Finally, after 90% reduction, fully-recovered micro-grains of 1 to 2$\mu$ in size are obtained.

Thus it would appear that by increasing the dislocation sinkage area, the annihilation of dislocations is increased and leads to increased softening. Fig. 3 suggests that after a reduction of 50%, an optimum minimum grain size is obtained. Based on this model it would appear that to achieve exceptional ductility, increased dislocation sinkage area; i.e. a very fine grain size is necessary.

Fig. 22 (X21,000) shows the micrograph of the as-rolled, 90% reduced metal with micro-grains of 1 - 2$\mu$ in size. The micro-grains are not quite equiaxed; they are slightly elongated in the direction of rolling. Very similar micrographs of Zn - $Zn_0$ alloys extrusions were obtained by Tromans and Lund (4), and electron diffraction of their extruded material showed that these grains were separated by high angle boundaries ($> 20)^{\circ}$.*

Thus the mechanism of this process seems to be: on straining, the as-rolled material at room temperature, a repetition of the dynamic softening process proposed for rolling occurs. In the steady-state region (Fig. 7), annihilation and reformation of dislocation arrays takes place at the equilibrium boundary-spacing. This generation and annihilation keep in balance and high uniform strains are obtained. It is now necessary to say why the grain size increases and becomes equiaxed during deformation, as shown in Fig. 24, and the following model is proposed based on an interpretation of Jonas et al (17) for the observed sub-grain growth which occurs during hot working. Equiaxed grains are obviously desirable and so, directly deformation starts, boundary migration occurs, by a continual breaking-up and reforming at an equilibrium spacing, converting the as-rolled, slightly-elongated grains to equiaxed ones. The original stable micro-grains are the result of the presence of particles, which pin the grain boundaries and prevent the sort of grain-growth observed in pure zinc at room temperature. As deformation occurs however, the particle spacing is increased along the tensile axis i.e., larger grains are 'allowed'. This, coupled with the lower energy-state of an equiaxed grain over an elongated grain provides for the formation of a larger, equiaxed grain-size. The approximate doubling of the grain size for a material elongated by about 100% suggests a final grain-size of the right order of magnitude.

---

*In this investigation electron diffraction studies to obtain the degree of misorientation between adjacent micro-grains was hampered by the background effect of the fine dispersion of lead particles present as impurities.

The hot working behaviour of materials with high stacking-fault energies and activation energies near that for self-diffusion and creep have been explained by theories involving dynamic recovery. Materials with low stacking-fault energies, and activation energies well above the self-diffusion values have been thought to involve dynamic recrystallization.

The activation energy for this process in the temperature range 20°C to 70°C, was found to be 21.5 ± 1 k cal/mole, a value very near the creep, self-diffusion and hot working values (17).

Wong et al (18) working on hot extrusion of aluminium, concluded that dynamic recovery was operating, based on transmission thin-film micrographs, showing sharp sub-boundaries which they describe as tight tangles of dislocation; the transmission thin-film micrographs obtained in this investigation are comparable with those of Wong et al. However, it seems unlikely that dislocation networks will be revealed in zinc thin-films at room temperature (0.43 Tm) and so their absence in Figures 22 and 24, is not surprising. Hayden et al (19), in their study of a super-plastic Ni-Fe-Cr alloy, suggested dynamic recovery as the mechanism; they failed to find extensive dislocation networks.

The extended plasticity observed in this work on commercial-purity zinc is due to dynamic recovery operating during deformation. Grain boundary sliding occurs on the surface and probably for a depth of a few microns below the surface, but this is the minor factor. However, grain boundary migration occurs during deformation, due to the increased spacing of the impurity particles along the tensile axis coupled with the lower energy state of equiaxed grains over elongated ones.

Deformation of Recrystallized Material

For the as-rolled, 90% reduction, recrystallized material, the strain-rate sensitivity exponent (m) of 0.06 was obtained. Fig. 5 shows the elongation versus percentage reduction. Speed of testing has virtually no effect on total elongation for the material rolled. The shape of the curve is judged to be due to grain size effect, i.e. 60% reduction before recrystallization giving the grain size for optimum ductility.

Fig. 23 is a transmission thin-foil micrograph of the as-rolled 90% reduction and recrystallized. Particles are evident at the grain boundaries and in the grains.

To see if the speed of testing is revealed by any difference in micro-structure specimens were tested at crosshead speeds of 0.02 in/min and 2 in/min. Fig. 14 shows the micrograph of the specimen tested at 0.02 in/min. Slip lines are clearly visible. Fig. 15 of the specimen tested at 2 in/min also exhibit slip lines, but on a finer scale. There is also evidence of duplex slip occurring in the specimen tested at the high speed.

In both cases fracture appears to be initiated at the grain boundary triple points and the crack progressing up the boundaries.

The vunerability of the grain boundaries to fracture is further increased by the presence of impurity particles in these regions.

Conclusions

(1) Heavily-rolled commercial-purity zinc is composed of micro-grains 1 - 2μ in diameter and remains in this condition at room temperature.

(2) The impurities - 0.8% lead, 0.05% cadmium and 0.02% iron, particularly the lead, in the form of finely-dispersed particles, are considered to stabilize these micro-grains and prevent recrystallization.

(3) The energy transferred to the zinc during rolling is expended in dynamic recovery which is manifested by the formation of these micro-grains.

(4) There is no evidence of slip in the as-rolled, 90% reduced material, while slip is observed in conventional, large grain, recrystallized material.

(5) The strain rate sensitivity exponent (m) for the as-rolled material, 90% reduction material is 0.2 and that for the recrystallized material is 0.06.

(6) The recrystallized material strain-hardens while the as-rolled material does not.

(7) Micrographic evidence from the recrystallized material shows widely spaced slip bands for specimens tested at a slow speed, and more closely spaced slip bands together with duplex slip for specimen tested at a fast speed. Fracture is initiated at the grain boundary triple points in both the cases.

(8) No slip was observed in the as-rolled material under various different conditions of testing. Fracture is initiated from the grain-boundary triple point.

(9) Surface examination shows that grain-boundary sliding and grain boundary rotation are occurring.

(10) Examination of thin foils and measurement of the activation energy of the process suggest dynamic recovery as the mechanism with a grain-size effect resulting from the presence of the particles and their spacing.

(11) Extended plasticity in commercial-purity zinc can thus be explained in terms of the simultaneous operation of both the currently popular mechanisms (sliding/migration and dynamic recovery), though dynamic recovery is the more important.

(12) Conclusions concerning mechanisms, and based solely on surface observation must be viewed with some suspicion.

References

1. R. Chadwick: J.I.M. 1933, vol. 41, p. 93.

2. J.A. Ramsey: J.I.M. 1951-52, vol. 80, p. 167.

3. W.H. McCarthy: Ph.D. Thesis, 1966, Stanford University.

4. D. Tromans and J.A. Lund. Trans. Am. Soc. Metals, 1966, Vol. 59, p. 672.

5. C.M. Sellars and W.J. McG. Tegart: Mun. Sci. de la Rev. Met. 1966, vol. 63, p. 731.

6. R.H. Johnson: Tube Investments Research Laboratories, Hinxton Hall, Cambridge, Tech. Memo. No. 292, p.1, 1967.

7. K. Detert: Recrystallization, grain growth and textures, papers presented at a Seminar of the Am. Soc. Metals, 1965.

8. D.L. Holt and W.A. Backofen: Trans - T.S.M. AIME, 1966, vol. 59, p. 755.

9. D. Lee and W.A. Backofen: Trans. T.S.M. AIME, 1966, vol. 239, p. 1034.

10. T.H. Alden: Acta Metallurgica, 1967, vol. 15, p. 469.

11. H.E. Clive and T.H. Alden: Trans. T.S.M. AIME, 1967, vol. 239, p. 710.

12. R.C. Gifkins: J.I.M. 1967, vol. 95, p. 373.

13. D.L. Holt: Trans. T.S.M. AIME, 1968, vol. 242, p. 25.

14. R.N. Stevens: Trans. T.S.M. AIME, 1966, vol. 236, p. 1762.

15. P. Gordon and R.A. Vandermeer: Recrystallization, grain growth and textures, papers presented at a Seminar of the Am. Soc. Metals, 1965.

16. W.J. McG. Tegart: College of Aeronautics, Cranfield, Note Mat. No. 14, 1967.

17. J.J. Jones, C.M. Sellars and W.J. McG. Tegart: Strength and Structure During Hot Working, a review prepared for Metallurgical Reviews, Dept. of Metallurgy University of Sheffield, 1968.

18. W.A. Wong, H.J. McQueen and J.J. Jonas. J.I.M. 1967, vol. 95, p. 129.

19. H.W. Hayden, R.C. Gibson, H.F. Merrick and J.H. Brophy: Trans. Am. Soc. Metals, 1967, vol. 60, p. 3.

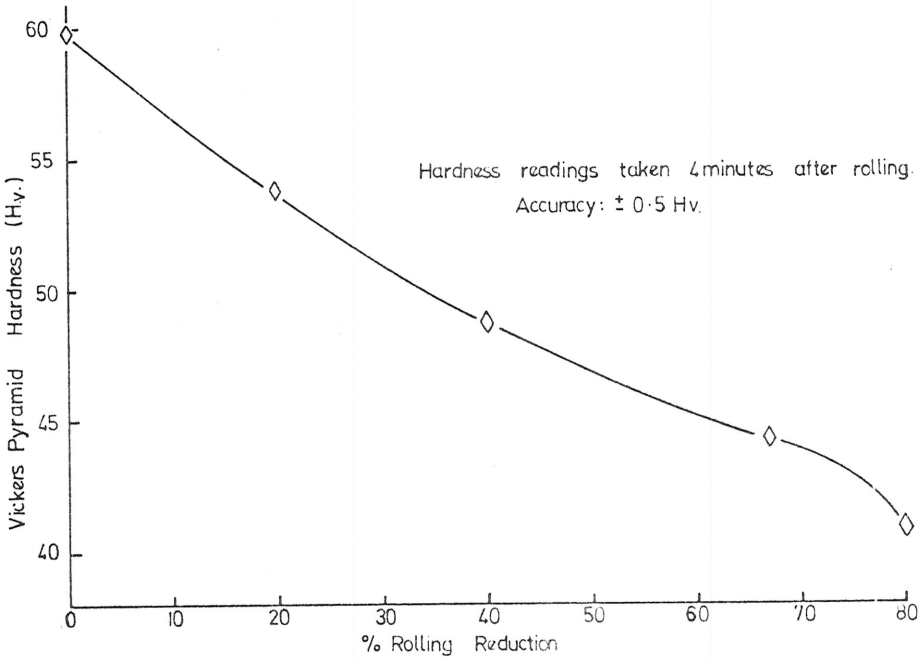
Hardness readings taken 4 minutes after rolling.
Accuracy: ± 0·5 Hv.
Vickers Pyramid Hardness (Hv.)
60
55
50
45
40
0
10
20
30
40
50
60
70
80
% Rolling Reduction

FIG 1

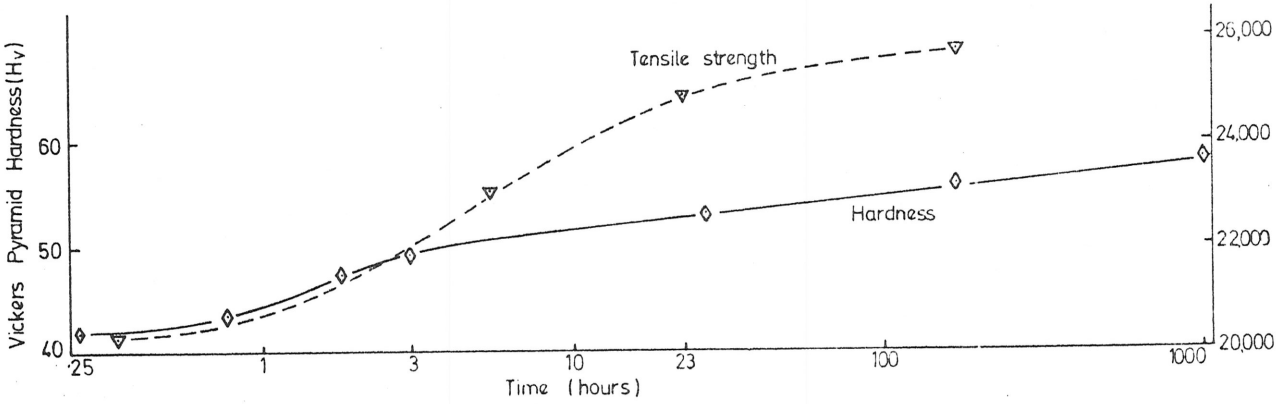
Tensile strength
Hardness
Vickers Pyramid Hardness (Hv)
60
50
40
26,000
24,000
22,000
20,000
·25
1
3
10
23
100
1000
Time (hours)

FIG. 2.

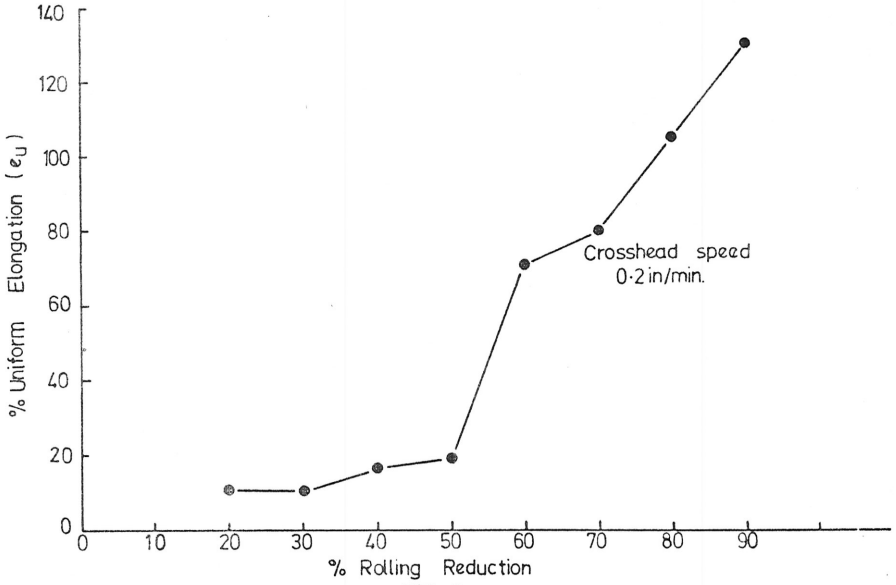


FIG. 3

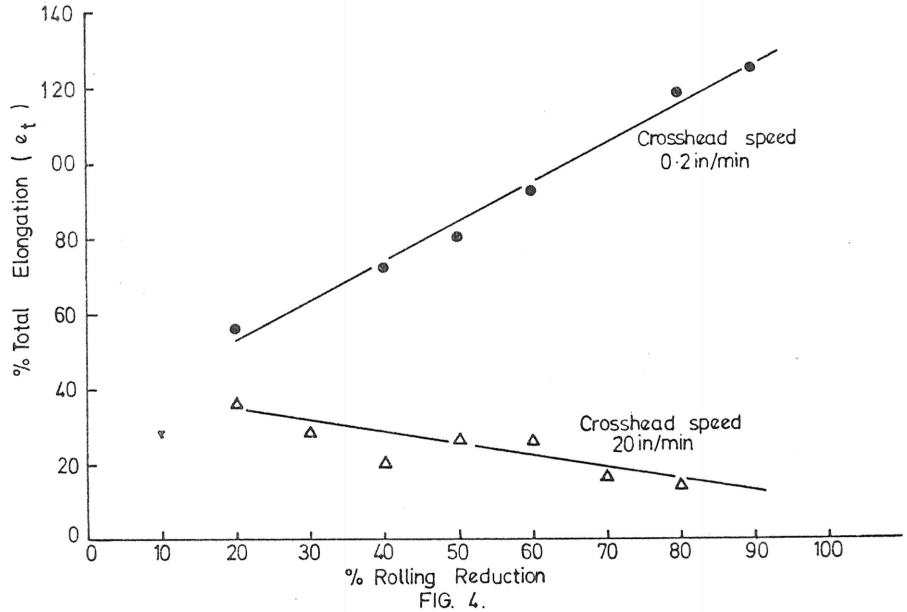


FIG. 4.

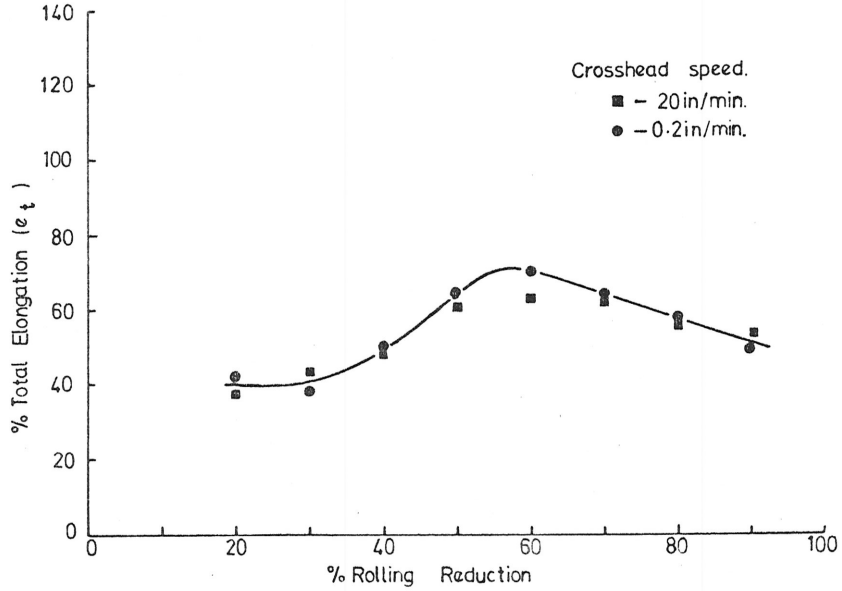


FIG. 5.

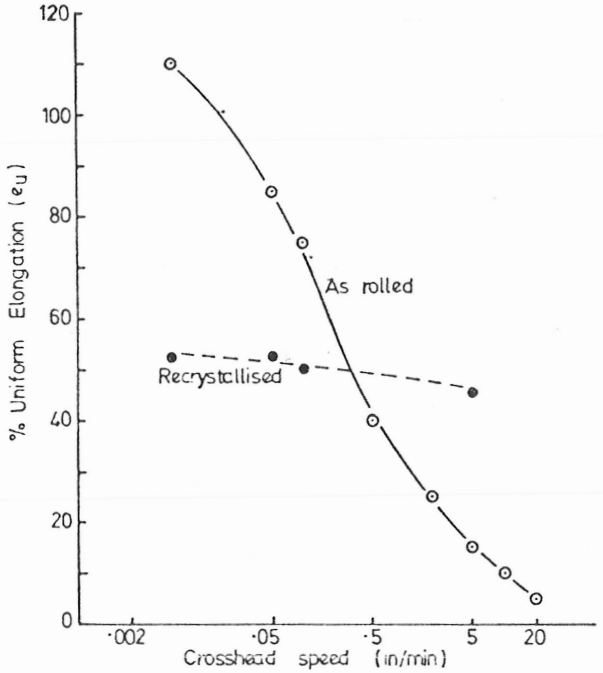
% Uniform Elongation ($e_u$)
120
100
80
60
40
20
0
As rolled
Recrystallised
·002
·05
·5
5
20
Crosshead speed (in/min)

FIG. 6.

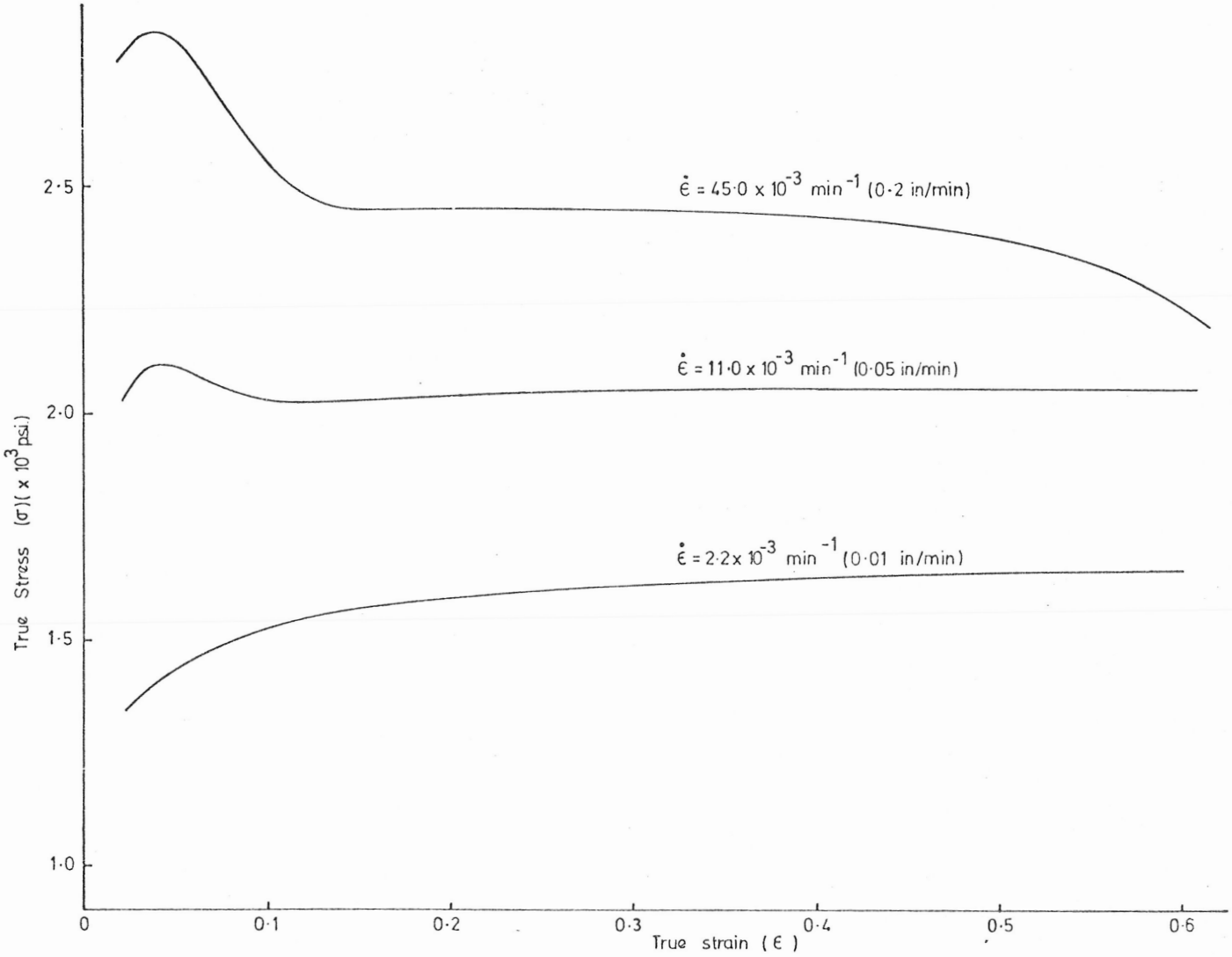
True Stress ($\sigma$)( x $10^3$psi.)
2·5
2·0
1·5
1·0
$\dot{\epsilon}$ = 45·0 x $10^{-3}$ $min^{-1}$ (0·2 in/min)
$\dot{\epsilon}$ = 11·0 x $10^{-3}$ $min^{-1}$ (0·05 in/min)
$\dot{\epsilon}$ = 2·2 x $10^{-3}$ $min^{-1}$ (0·01 in/min)
0
0·1
0·2
0·3
0·4
0·5
0·6
True strain ($\epsilon$)

FIG. 7.

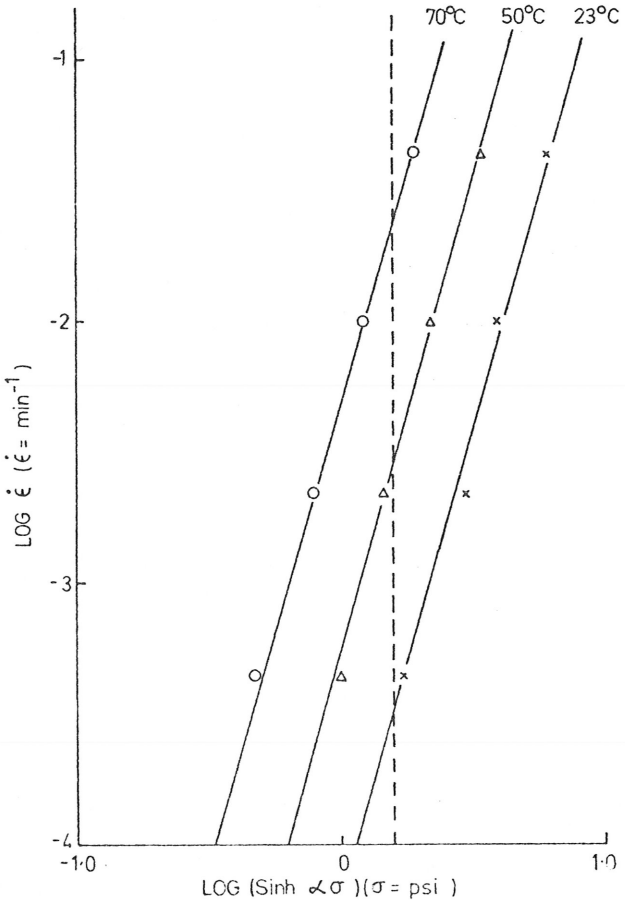
70°C
50°C
23°C
-1
-2
-3
-4
-1·0
0
1·0
LOG $\dot{\epsilon}$ ($\dot{\epsilon}$ = min$^{-1}$)
LOG (Sinh $\alpha\sigma$)($\sigma$ = psi)

FIG. 8.

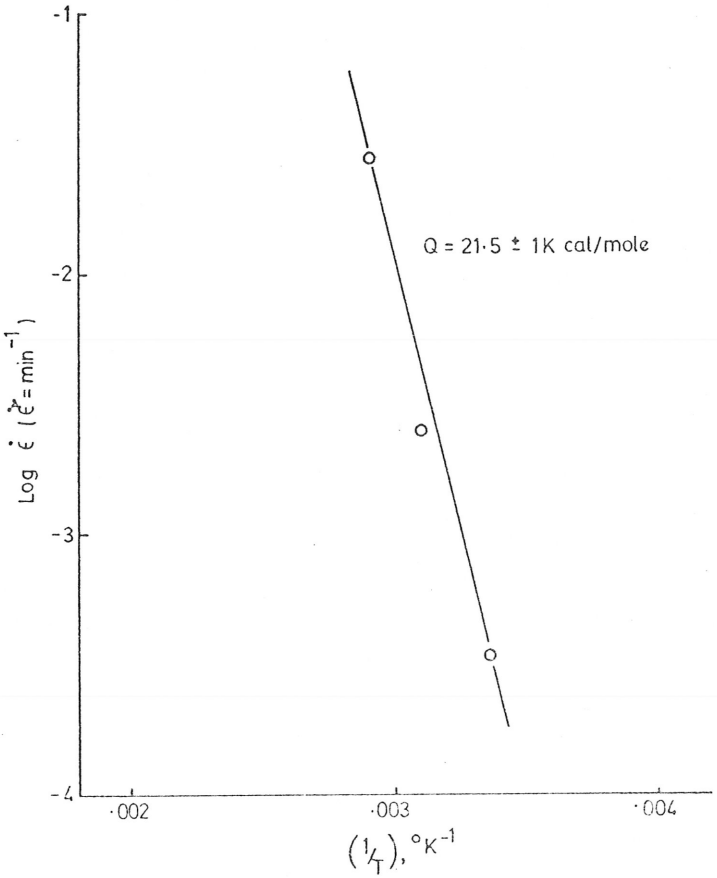
Q = 21·5 ± 1K cal/mole
-1
-2
-3
-4
·002
·003
·004
Log $\dot{\epsilon}$ ($\dot{\epsilon}$ = min$^{-1}$)
$(1/T)$, °K$^{-1}$

FIG. 9.

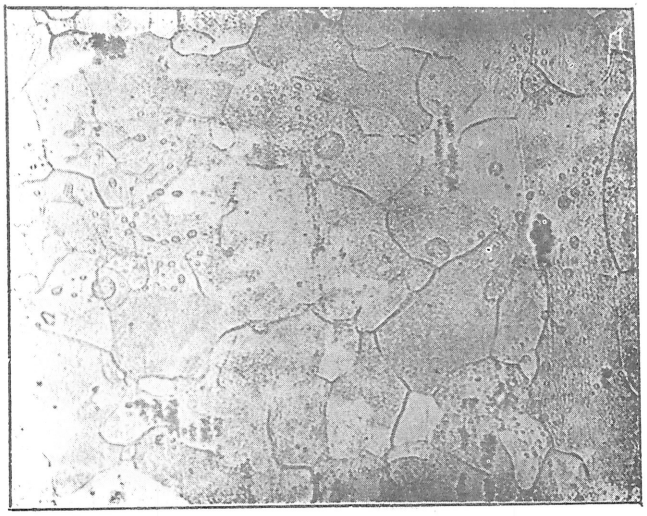

Mag. x 480
Starting Material

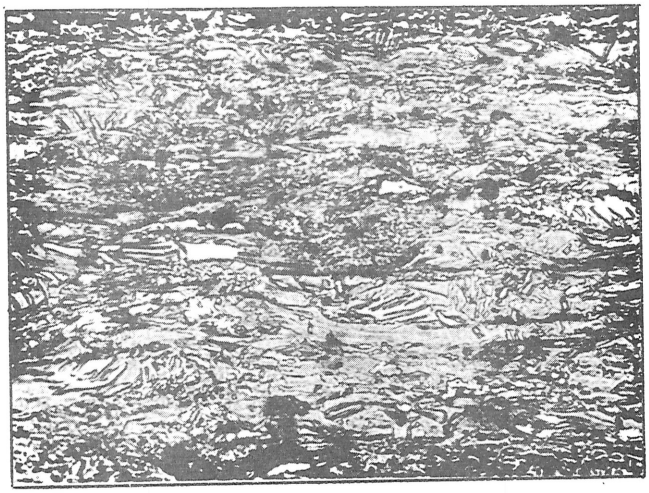

Rolled 40%

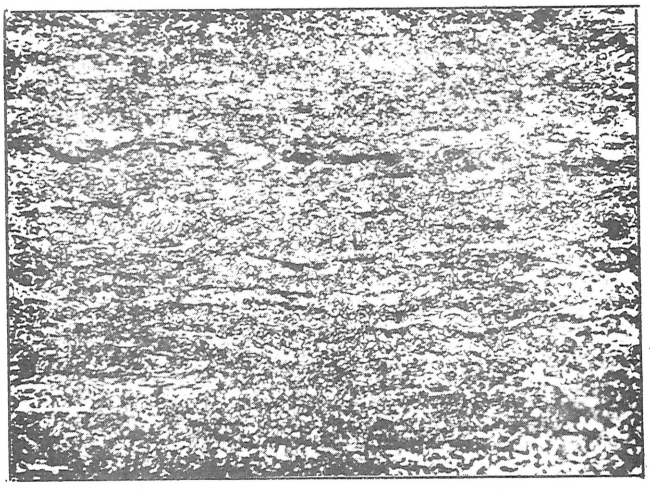

Rolled 80-90%

Fig. 10 - All longitudinal sections.

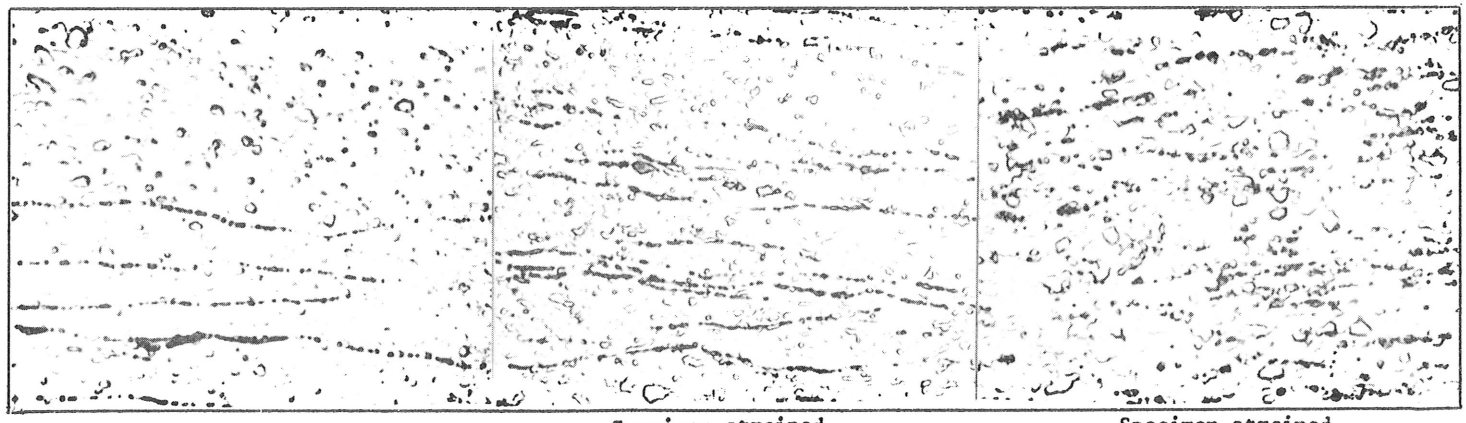

Mag. x 1000

Grip ends

Specimen strained at 20 in/min.

Specimen strained at 0.2 in/min.

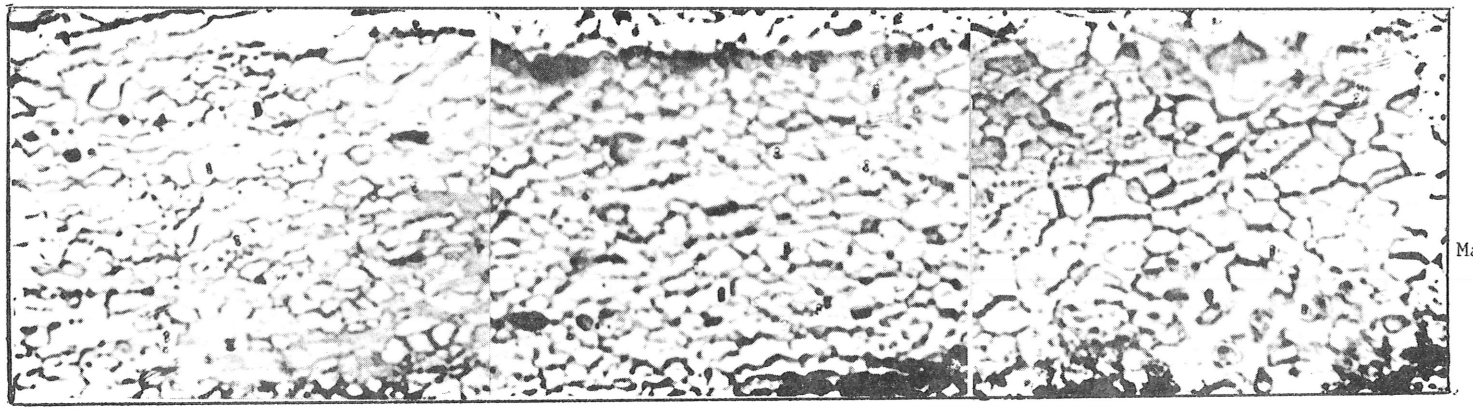

Mag. x 3000

Grip ends

Specimen strained at 20 in/min.

Specimen strained at 0.2 in/min.

Fig. 11 - All longitudinal sections.

Rolled 90% Reduction and
Recrystallized at 200°C
for 15 mins.

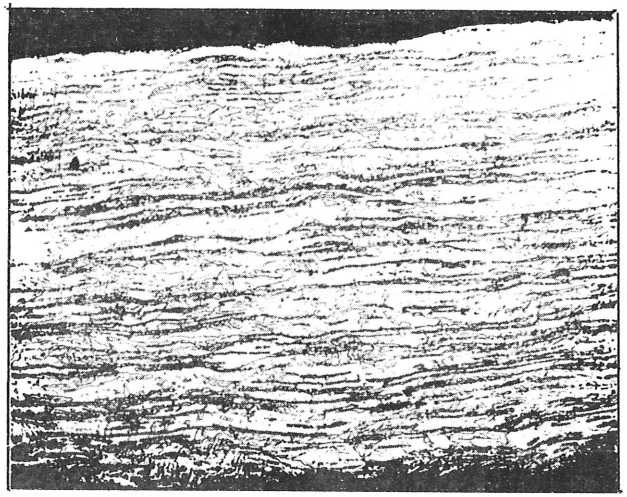

Specimen Strained at 20in/min.

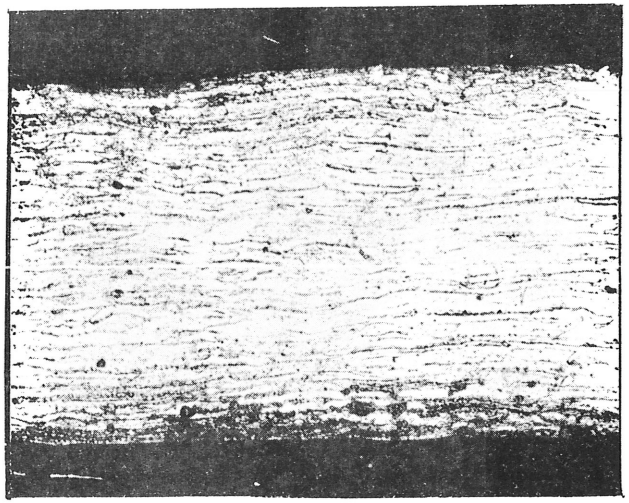

Specimen Strained at 0.2in/min.

Fig. 12 - All longitudinal sections.
Mag x 200.

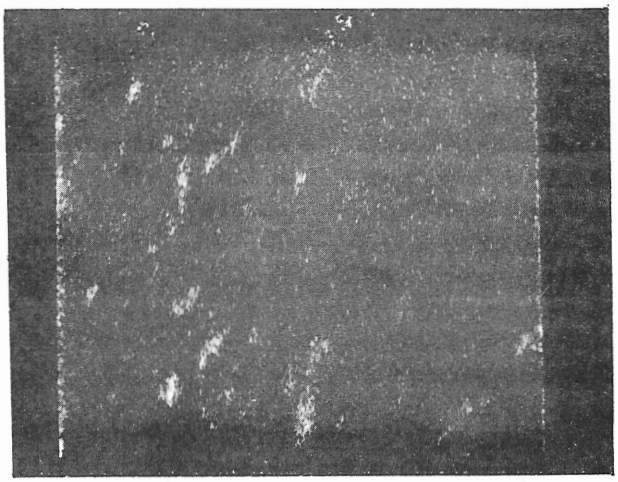

100 μ sq

Fig. 13 - As rolled 90% reduction material showing dispersion of lead in a zinc matrix.

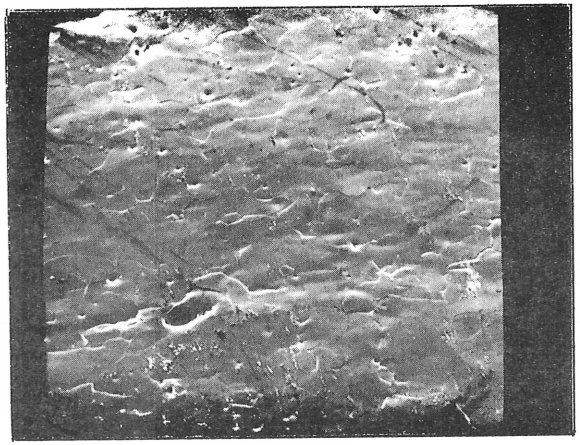

Mag. x 500

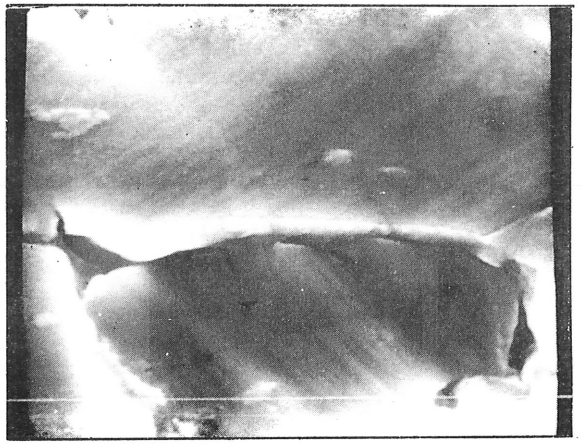

Mag. x 4500

Fig. 14 - Recrystallized and strained 5% at 0.02 in/min.

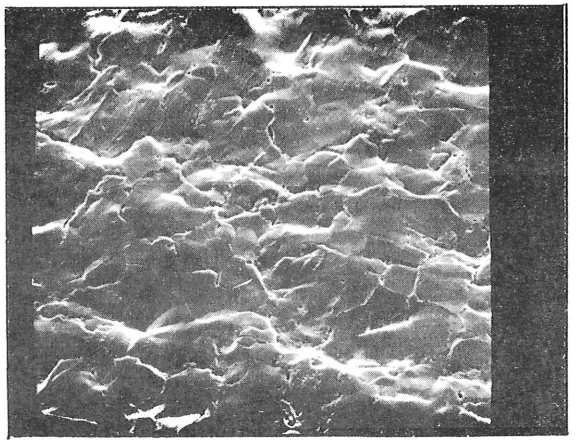

Mag. x 500

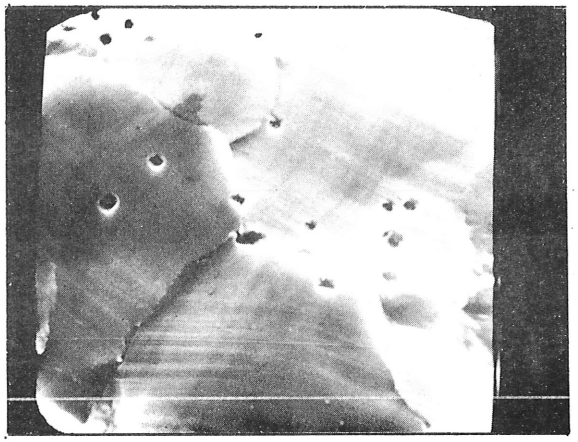

Mag. x 4500

Fig. 15 - Recrystallized and strained 50% to fracture at 2 in/min.

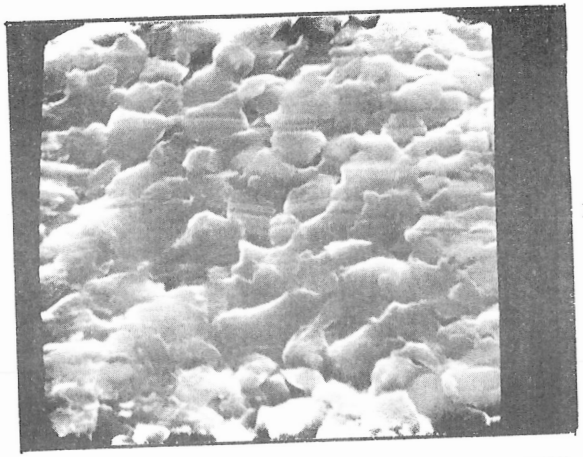

Mag. x 10,000

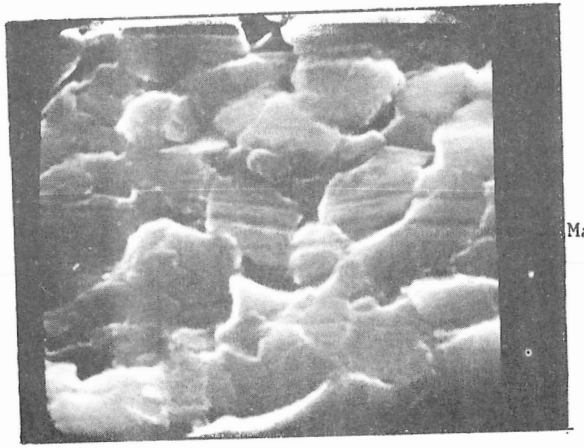

Mag. x 20,000

Fig. 16 - As rolled 90% reduction and strained 50% at 2 in/min.

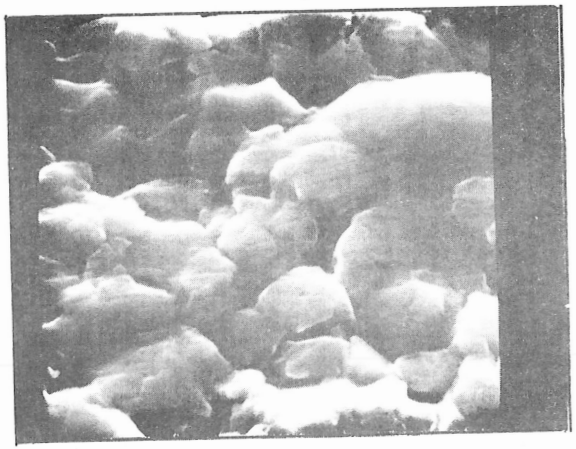

Mag. x 10,000

Mag. x 20,000

Fig. 17 - As rolled 90% reduction and strained 100% at 0.02 in/min.

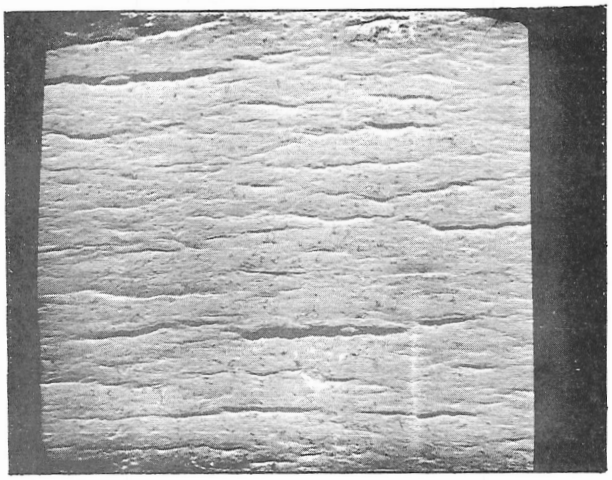

Mag x 100

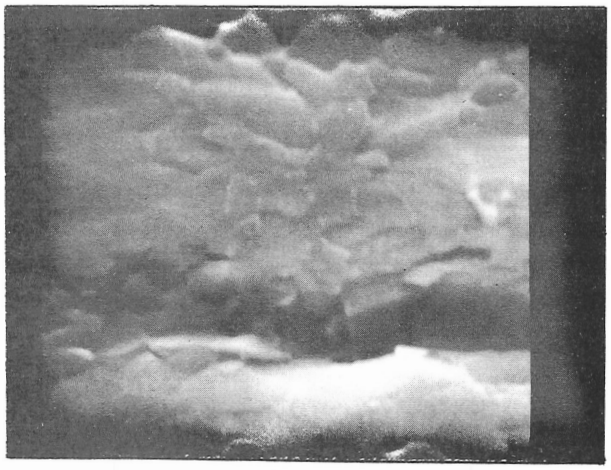

Mag x 10,000

Fig. 18 - As rolled 90% reduction and strained to fracture ($e_t$ = 25%) at 20 in/min.

Mag x 12,800

strained at -196°C to fracture ($e_t$ = 0%)

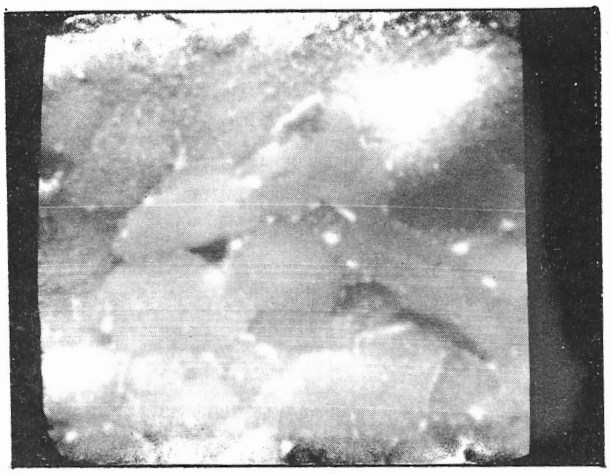

Mag x 8400

strained at -55°C to fracture ($e_t$ = 5%)

Fig. 19 - Both specimens strained at 0.2 in/min.

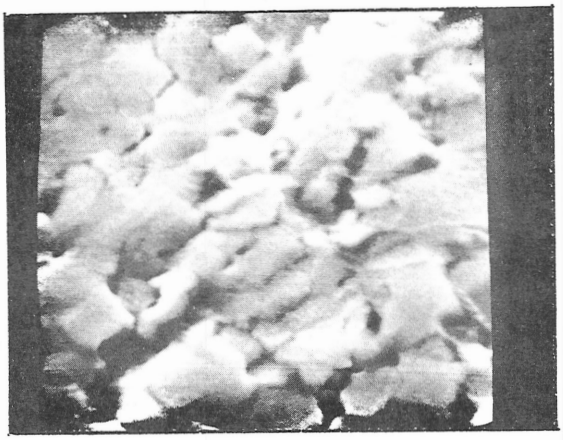

Mag x 10,000 strained at $0^{o}C$ to fracture ($e_t$ = 30%)

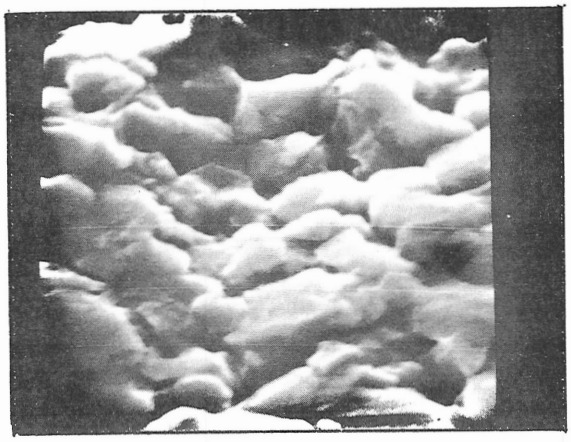

Mag x 10,000 strained at $20^{o}C$ to fracture ($e_t$ = 75%)

Mag x 10,000 strained at $70^{o}C$ to fracture ($e_t$ = 160%)

Fig. 20 - All specimen strained at 0.2 in/min.

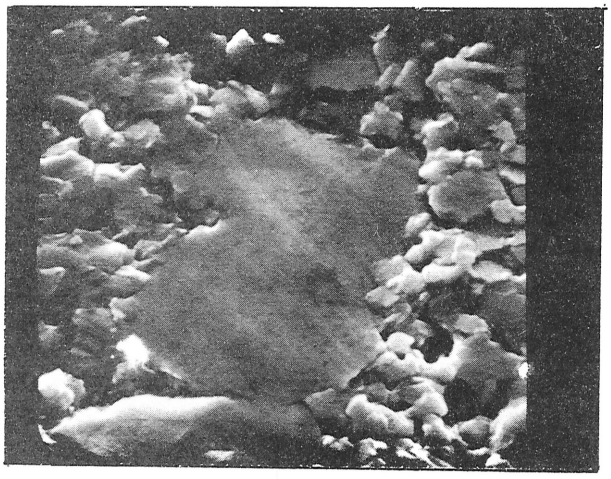

Mag x 5040

Fig. 21 - As rolled 90% reduction and strained at 0.2 in/min.

Mag x 21,000

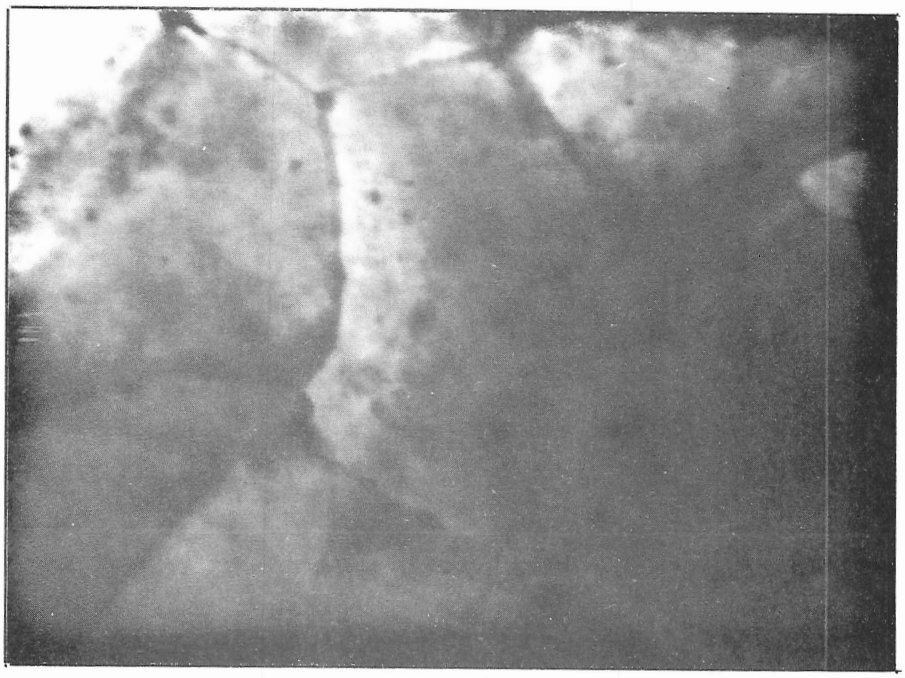

Mag x 42,000

Fig. 22 - As rolled 90% reduction material.

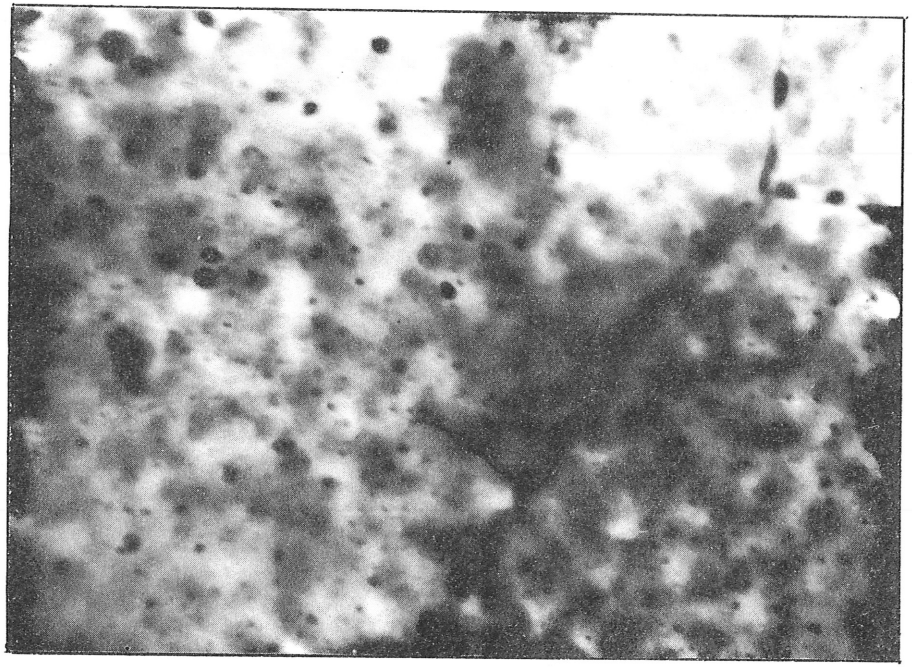

Mag x 42,000

Fig. 23 - Recrystallized material.

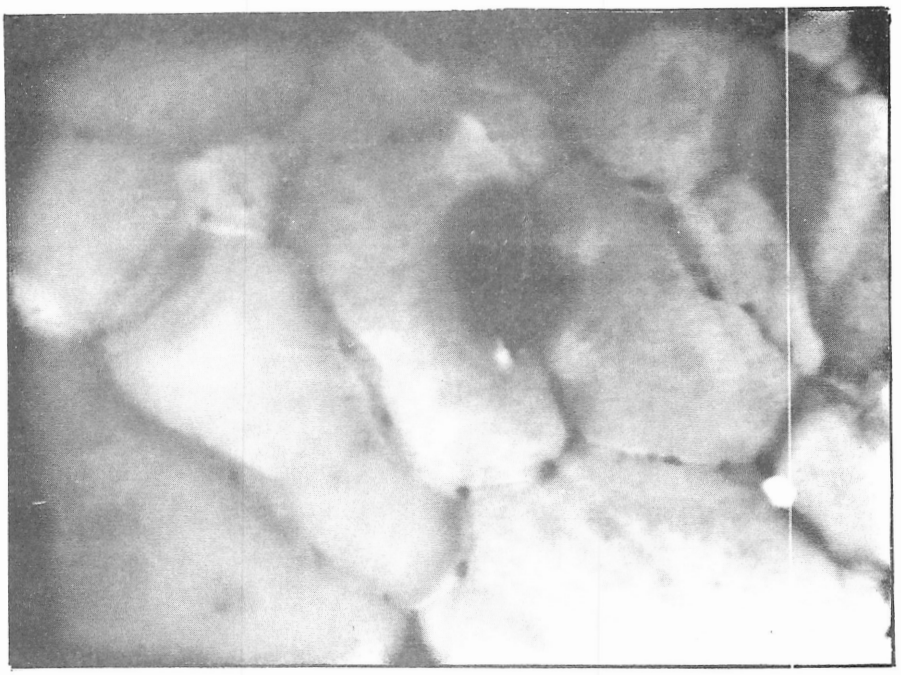

Mag x 21,000

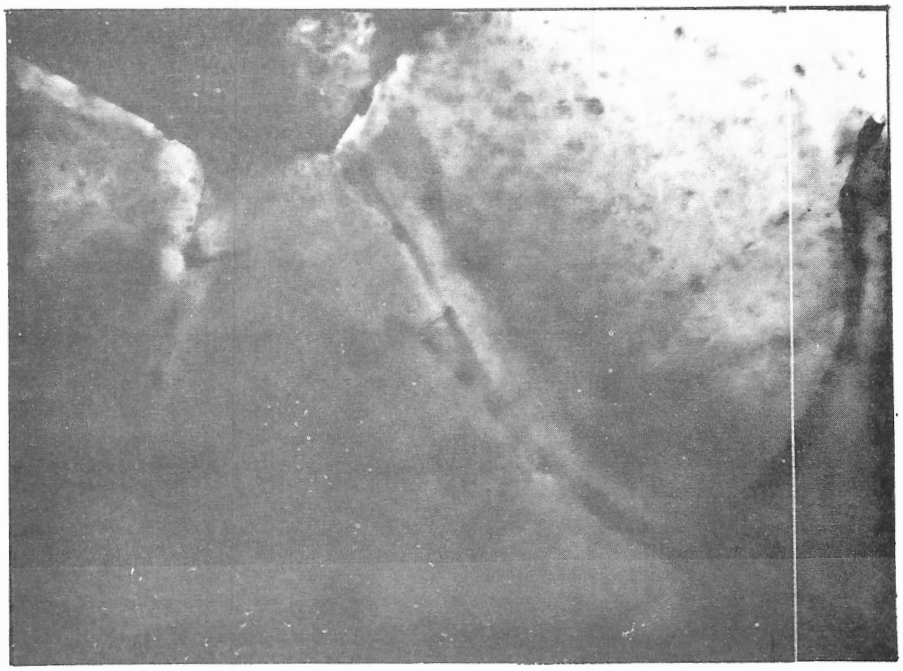

Mag x 42,000

Fig. 24 - As rolled 90% reduction and strained 200% at 0.002 in/min.